2018 5th International Workshop on Compressed Sensing applied to Radar, Multimodal Sensing, and Imaging (CoSeRa)

# Reconstruction of Rigid Body with Noncompensated Acceleration After Micro-Doppler Removal

M. Brajović[1], I. Stanković[1,2], C. Ioana[2], M. Daković[1], L. Stanković[1],
[1] Faculty of Electrical Engineering, University of Montenegro, 81000 Podgorica, Montenegro
[2] GIPSA Lab, Grenoble INP, Université Grenoble Alpes, 38000 Grenoble, France

***Abstract*—The micro-Doppler (m-D) effect, commonly appearing in ISAR/SAR radar images, is caused by fast moving reflectors of the target. This effect can significantly impact the readability of radar images. Recently, an algorithm for the separation of the m-D from the target rigid body has been proposed, based on the short-time Fourier transform (STFT) and the L-statistics. For cases of targets with noncompensated acceleration, this approach is modified to use the Local Polynomial Fourier transform (LPFT). In our recent paper, we have proposed a simple algorithm for the search of acceleration compensation parameter in the LPFT (chirp-rate parameter). In this paper we deal with the reconstruction of the target's rigid body after the L-statistics based removal of the micro-Doppler, for the case of noncompensated target's motion. The reconstruction is performed based on compressive sensing and sparse signal processing theory.**

***Keywords*—ISAR, Compressive sensing, DFT, Sparse signals, Signal reconstruction***

## I. Introduction

Radar imaging is an important application field of the time-frequency (TF) signal analysis [1]- [11]. The presence of fast rotating or vibrating parts of the target causes the appearance of the micro-Doppler (m-D) effect [1]- [9]. In order to focus the radar images and improve the readability [1]- [9], significant research efforts have been conducted towards the problem of rigid body and m-D components separation in the received radar signals. Micro-Doppler signal parts are highly nonstationary. In the case of rotating and vibrating target reflectors, it is commonly modeled by sinusoidally frequency modulated (FM) components. For the compensated acceleration, rigid body consists of stationary components. The noncompensated movement of rigid body reflectors is commonly modeled with linear FM components in the received radar signal [1].

The separation of rigid body from the m-D, based on the short-time Fourier transform (STFT) and the L-statistics, has been studied recently. [1]. The state-of-the-art technique presented in [1] is very efficient, producing highly concentrated rigid body after the m-D removal. Recently emerging areas of compressed sensing and sparse signal processing [11]- [18] also provided techniques for the reconstruction of stationary rigid body [11], [13]. The reconstruction of noncompensated rigid body acceleration has been considered in [1], [12]. Therein, the Local Polynomial Fourier Transform (LPFT) is proposed as the initial TF representation. However, the application of this representation requires the estimation of the chirp-rate parameter serving for the movement compensation, which is a priori unknown [1]. This value cannot be estimated based on the original signal. Namely, it was shown that the L-statistics-based approach must be involved in the parameter search procedure.

Recently, we have proposed a new search procedure for the acceleration compensation parameter [3]. It is based on concentration measure [12] of the LPFT, calculated after applying the L-statistics in each iteration of the algorithm. The motivation was the high numerical complexity of the direct search. In this paper, we deal with the reconstruction of the rigid body with uncompensated acceleration using compressed sensing (sparse signal processing) techniques in conjunction with the described parameter search procedure [3].

The background theory is presented in Section II. The STFT-based rigid body separation algorithm is presented in Section III. In this Section, the algorithm for the acceleration compensation parameter is also presented. The rigid body reconstruction based on sparse signal processing concepts is described in Section IV. Numerical results are presented in Section V.

## II. Background theory and the signal model

Consider a continuous wave (CW) radar transmitting signals in form of $N$ coherent chirps. If the target distance is denoted by $d(t)$, and $c$ is the speed of light, then the signal reflected from the target is delayed for $t_d = 2d(t)/c$ with respect to the transmitted signal. Standard preprocessing operations are assumed in the model (such as, for example, signal demodulation to the baseband) [1].

As it is commonly done in the radar literature [1], aiming to analyze cross-range nonstationarities in the radar imaging, only the Doppler part of the received signal of a point target in the continuous dwell time will be considered

$$s(t) = \sigma e^{\frac{j2d(t)\omega_0}{c}}, \tag{1}$$

where the target reflection coefficient is denoted by $\sigma$, and $\omega_0$ is the radar operating frequency. It is assumed that the pulse repetition time is $T_r$ with $N_c$ samples within each chirp, and that the coherence integration time (CIT) is $T_c = NT_r$.

The Doppler part of the received signal, corresponding to the rigid body, can be modeled with complex sinusoids [1]. However, in the noncompensated target acceleration case the rigid body would induce linear FM components [1]. Targets usually consist of some fast moving vibrating and rotating parts. They cause the appearance of additional nonstationary components in the received signal. These components are widely known as the the micro-Doppler. Rotating or vibrating reflectors produce m-D modeled with sinusoidal FM signals.

For an arbitrary movement of the reflectors, this model is more complex. For systems of point scatterers, the received signal is modeled as a sum of individual scatterer responses. The general model assuming the rigid body consisted of $K$ points, and m-D caused by $D$ reflectors [1] is given as

$$s(n) = \sum_{i=1}^{K} \sigma_{B_i} e^{jy_{B_i} n} + \sum_{i=1}^{D} \sigma_{R_i} e^{jA_{R_i} \sin(\omega_{R_i} n + \Theta_i)}, \quad (2)$$

where $n = 0, \ldots, N-1$, $\sigma_{B_i}$ and $\sigma_{R_i}$ are reflection coefficients of the rigid body and rotating reflectors, $y_{B_i}$ corresponds to the position of the rigid body reflector, $A_{R_i}$ is proportional to the distance from the rotating reflector to the center of rotation. Angle frequencies $\omega_{R_i}$ are proportional to the rotating rate of the $i$th m-D reflector. Detailed explanations of the presented signal model followed by corresponding ISAR/SAR geometry schemes can be found in [1].

## III. The separation of the rigid body and micro-Doppler

The efficiency of the method for the separation of rigid body and m-D, presented in [1], is not dependent on the assumed m-D model, and for arbitrarily highly nonlinear motion of m-D points excellent results are also expected. Further, an appropriate sampling of the received signal $s(t)$ is assumed, and the processing is performed on signal's discrete samples $s(n)$. Rigid body components are stationary, but due to the highly variable frequency content of the m-D, it is impossible use the classical Fourier transform based analysis of these signals. Therefore, time-frequency signal analysis approaches are commonly exploited in this context. The ability of a transform (time-frequency representation) $TFR(n,k)$ to concentrate the signal content in the smallest possible number of transform coefficients with significant values is quantitatively determined by concentration measures [12], commonly obtained by measuring the transformation spread. This idea comes from counting non-zero values using $\ell_0$-norm of the transformation. However, due to its sensitivity, norms of the form $\mathcal{M}_p^p = (\sum_n \sum_p |TFR(n,k)^{\frac{1}{p}}|)^p$ are engaged more commonly. The most widely used norm is obtained for $p = 1$. Being known as $\ell_1$-norm, it is used in the recent compressive sensing context [11]. This form of concentration measure is assumed in this paper. The short-time Fourier transform (STFT) of the analyzed signal is defined as

$$STFT(n,k) = \sum_{m=0}^{N-1} s(m) w(m-n) e^{-j2\pi mk/N}, \quad (3)$$

where the window function $w(m)$ is used for the localization of the frequency content. In this STFT form, $w(n) \neq 0$ for $-M/2 \leq m \leq M/2-1$ and it is zero-padded up to the signal length $N$. The original FT concentration can be obtained from (3) calculating

$$\begin{aligned} S(k) &= \sum_{n=M/2}^{N-M/2} STFT(n,k) \\ &= \sum_{m=0}^{N-1} s(m) \left[ \sum_{n=M/2}^{N-M/2} w(m-n) \right] e^{-j2\pi mk/N}. \end{aligned} \quad (4)$$

As $\sum_{n=M/2}^{N-M/2} w(m-n) \approx const$ holds, the resulting window it is very close to a rectangular case, as is constant during the CIT interval, (except for a small transition for ending $M/2$ points at both sides). Therefore, (4) can be considered as the Fourier transform of the analyzed signal, with concentration close to the Fourier transform calculated with a full range rectangular window. The m-D can be removed from the $STFT(n,k)$ sorting its values over time, and removing a certain percent of highest values. Summing the remaining points over the frequency, a FT approximation of the rigid body is obtained.

### A. Micro-Doppler removal in the case of stationary rigid body

In the case of a stationary rigid body, the STFT-based separation of the rigid body and the m-D is done as follows. For each frequency index $k$, we denote the corresponding set of STFT points as

$$\mathbf{S}_k = \{STFT(n,k),\ n = M/2, ..., N - M/2\}. \quad (5)$$

Sorting elements of this set (over the time index), an ordered set $\mathbf{\Psi}_k$ is formed, with elements $\Psi_k(n_i) \in \mathbf{S}_k$, $n_i \in \{M/2, \ldots, N-M/2\}$. These elements, for each $k$ satisfy

$$|\Psi_k(n_1)| \leq |\Psi_k(n_2)| \leq \cdots \leq |\Psi_k(n_{N-M})|. \quad (6)$$

The L-statistics based separation of the rigid body from the m-D assumes that $N_U$ highest and $N_D$ lowest elements are removed from $\mathbf{\Psi_k}$, for each $k$. It is a column vector of size $M \times 1$. If $U$ is the percent of eliminated highest elements, and $D$ of eliminated lowest elements, then $N_U = \text{int}[(N-M)(1-U)/100]$ highest and $N_D = \text{int}[(N-M)(1-D)/100]$ lowest elements is removed. Altogether $Q = D + U$ percent of STFT points is removed. For given $k$, the set of available positions is $\mathbb{L}_k$ and it is the subset of $\{n_1, n_2, \ldots, n_{N-M}\}$. Sets $\mathbb{L}_k$ for each $k = 0, \ldots, M-1$ form set $\mathbb{N}_A$ containing indexes $(n_i, k_i)$ of available (retained) time-frequency points. As

$$S_\Psi(k) = \sum_{n=M/2}^{N-M/2} STFT(n,k) = \sum_{i=1}^{N-M} \Psi_k(n_i) \quad (7)$$

obviously holds, then based on on the obtained subset $\mathbb{L}_k$ of $\{n_1, n_2, \ldots, n_{N-M}\}$, the L-estimate

$$S_L(k) = \sum_{n \in \mathbb{L}_k} STFT(n,k) \quad (8)$$

can be calculated. It is a simple approach to approximate the rigid body components, after the m-D is removed. Stationary rigid body components are, for given frequency, present in all time instants. On contrary, m-D components' frequency is time-dependent. Therefore, summing over time the STFT points, values belonging to the rigid body peak will be summed in phase. Therefore, a highly concentrated peak in the FT domain is produced for each rigid body component. The low concentrated m-D components remaining after the removal of $Q\%$ of STFT points for each $k$ will be summed up by different random phases, thus averaging out. A more detailed discussion of this result is presented in [1].

### B. Noncompensated rigid body acceleration

Accelerating target motion produces linear FM signals corresponding to the rigid body reflectors [1]. In that case, in the received radar signal model (2), stationary rigid body components are replaced with linear FM terms, having an unknown chirp-rate $a$. The simplified case of parallel linear FM components will be considered. The resulting rigid body becomes non-stationary, and the procedure presented in previous section would eliminate significant parts of the rigid body. The LPFT of the following form

$$LPFT_{\alpha}(n,k)=\sum_{m=-M/2}^{M/2-1} s(n+m)w(m)e^{-j2\pi[\frac{m}{M}k+\alpha(\frac{m}{M})^2]},$$

can be exploited in order to determine the optimal chirp rate $\alpha_{opt}=a$. As the unknown dechirping parameter cannot be estimated based on the original signal, L-estimation will be involved in the following procedure, as described in Section III-A. The approach is originally presented in [3].

**Step 0:** Initialize $\nabla = N/2$ and $\alpha^{(0)}=0$.
Then, repeat Steps 1-4 until a stopping criterion is met:

**Step 1**: Calculate:

$$LPFT_{\alpha^+}(n,k) = \sum_{m=-M/2}^{M/2-1} s(n+m)w(m)e^{-j2\pi[\frac{m}{M}k+(\alpha+\nabla)(\frac{m}{M})^2]},$$

$$LPFT_{\alpha^-}(n,k) = \sum_{m=-M/2}^{M/2-1} s(n+m)w(m)e^{-j2\pi[\frac{m}{M}k+(\alpha-\nabla)(\frac{m}{M})^2]},$$

**Step 2**: Apply the L-statistics as described in Section III on both $LPFT_{\alpha^+}(n,k)$ and $LPFT_{\alpha^-}(n,k)$. Starting from given sets of LPFT points

$$\mathbf{L}_k^{\pm}(n)=\{LPFT_{\alpha^{\pm}}(n,k),\ n=M/2,...,N-M/2\}$$

sort the values of these sets over $n$ to obtain new, ordered sets of elements, $\Psi_k^+(n_i)\in\mathbf{L}_k^+(n)$, and $\Psi_k^-(n_j)\in\mathbf{L}_k^-(n)$, $n_i,n_j\in\{M/2,\dots,N-M/2\}$ satisfying, for given $k$: $|\Psi_k^+(n_1)|\le|\Psi_k^+(n_2)|\le\cdots\le|\Psi_k^+(n_{N-M})|$ and $|\Psi_k^-(n_1)|\le|\Psi_k^-(n_2)|\le\cdots\le|\Psi_k^-(n_{N-M})|$.

Highest $N_Q$ values from $\mathbf{\Psi}_k^+(n_i)$ and $N_Q$ values from $\mathbf{\Psi}_k^-(n_j)$ are omitted, where $N_Q=\text{int}[(N-M)(1-Q)/100]$ and Q is the percent of omitted values.

Based on the obtained subsets $L_k^+$ and $L_k^-$ of $\{n_1,n_1,\dots,n_{N-M}\}$, calculate

$$S_L^+(k)=\sum_{n\in L_k} LPFT_{\alpha^+}(n,k), \tag{9}$$

$$S_L^-(k)=\sum_{n\in L_k} LPFT_{\alpha^-}(n,k). \tag{10}$$

**Step 3**: Approximate the concentration measure [12] gradient as the difference of the form:

$$\nabla=\sum_{k=0}^{M-1}|S_L^+(k)|-\sum_{k=0}^{M-1}|S_L^-(k)|. \tag{11}$$

**Step 4**: Update the parameter in the gradient direction:

$$\alpha^{(l+1)}=\alpha^{(l)}-\mu\nabla. \tag{12}$$

The resulting parameter $\alpha$ is further used to demodulate the signal and apply the m-D removal and rigid body reconstruction algorithm presented in Section III. In numerical examples, step $\mu=\frac{M}{N_Q}$ is used. The iteration index is denoted by $l$. Detailed analysis of the optimal step value is part of our further research.

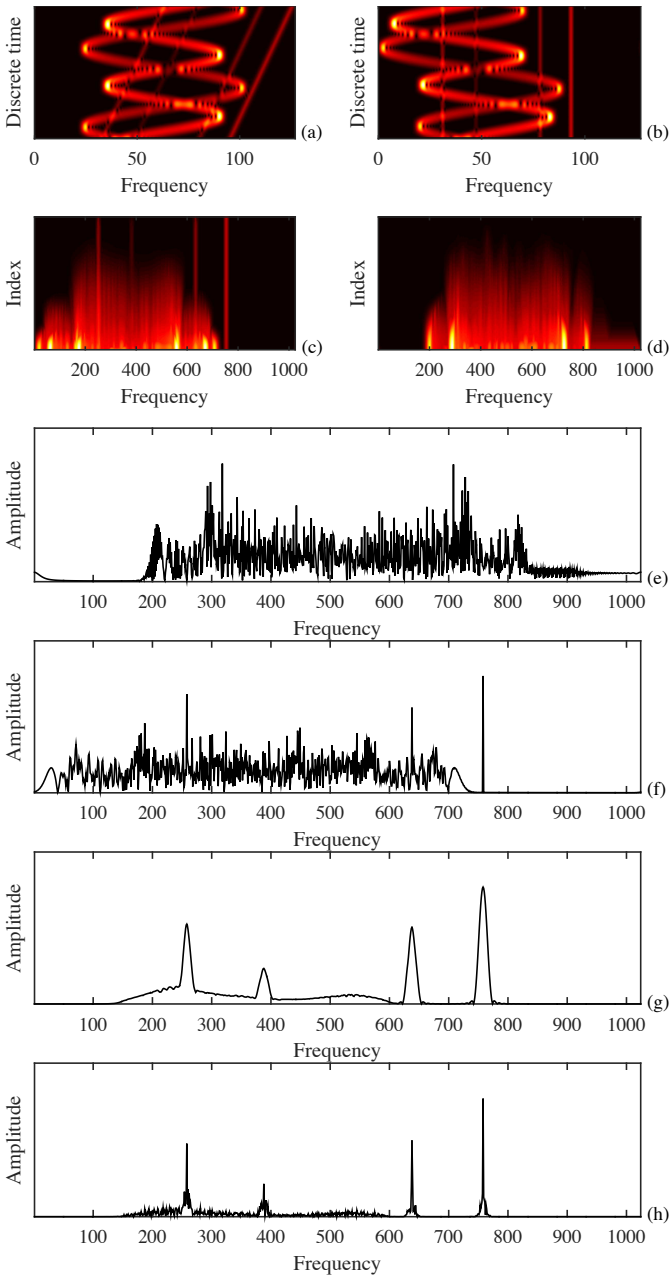


Fig. 1. Rigid body and m-D separation when the rigid body acceleration is not compensated. (a) The STFT of the original signal, calculated according to (3). (b) The STFT of the signal demodulated with suitable $\alpha$ using the presented algorithm. (c) Sorted values of the original signal. (d) Sorted values of the STFT shown in subplot (b). (e) FT of the original signal. (f) FT of the dechirped signal. (g) FT obtained summing lowest 40% of absolute values of the dechirped signal STFT over time. (h) FT obtained summing lowest 40% of the dechirped signal STFT over time, using (8).

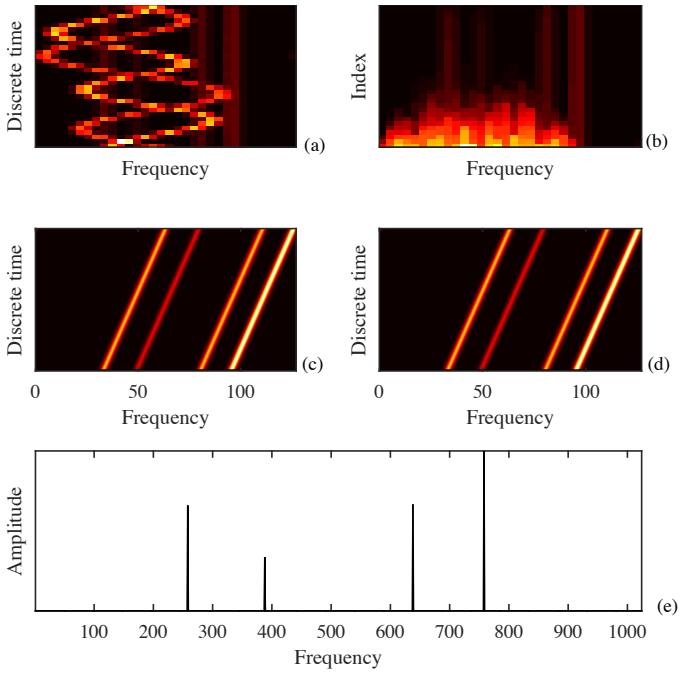


Fig. 2. Non-overlapped STFT as the basis for the CS-based rigid body recontruction. (a) The STFT of the appropriately dechirped signal (using parameter $\alpha$ produced by the presented searching algorithm), calculated according to (13). (b) The STFT values sorted over the time index. (c) STFT of the original rigid body defined in (22). (d) The STFT of the reconstructed rigid body calculated using (3) over the inverse DFT of coefficients shown in (e). This signal is modulated with $\alpha$ to form the original rigid body. (e) DFT coefficients corresponding to the stationary components of the dechirped rigid body, reconstructed using the presented CS-based approach.

## IV. The Rigid Body Reconstruction

Denote the vector containing properly demodulated signal

$$s_\alpha(n) = s(n)e^{-j2\pi\alpha(n/N)^2}$$

samples with $\mathbf{s}_\alpha = [s_\alpha(0), s_\alpha(1)..., s_\alpha(N-1)]$. If $\mathbf{W}_M$ is an $M \times M$ discrete Fourier transform (DFT) matrix with elements $\exp(-j2\pi mk/M)$, then the STFT of the demodulated signal (the second form considered in this paper)

$$STFT_\alpha(n,k) = \sum_{m=0}^{N-1} s(n+m)w(m)e^{-j2\pi mk/N} \quad (13)$$

has the following matrix form

$$\mathbf{STFT}_\alpha = \begin{bmatrix} \mathbf{W}_M & \mathbf{0} & \cdots & \mathbf{0} \\ \mathbf{0} & \mathbf{W}_M & \cdots & \mathbf{0} \\ \vdots & \vdots & \ddots & \vdots \\ \mathbf{0} & \mathbf{0} & \cdots & \mathbf{W}_M \end{bmatrix} \mathbf{s}_\alpha$$

$$\mathbf{STFT}_\alpha = \mathbf{W}\mathbf{s}_\alpha = \mathbf{W}\mathbf{W}_N^{-1}\mathbf{S}_\alpha, \quad (14)$$

where $\mathbf{S}_\alpha$ is the vector of DFT coefficients calculated for the full length signal and for unity rectangular window. Here, we assume that the $STFT_\alpha(n,k)$ is calculated at points $0,\ M,\ 2M, \ldots, N-M$. All the STFT values are combined into one vector

$$\mathbf{STFT}_\alpha = [\mathbf{STFT}_M(0)^T, \ldots, \mathbf{STFT}_M(N-M)^T]^T. \quad (15)$$

For each considered instant, STFT vectors are

$$\mathbf{STFT}_M(n) = [STFT(n,0), \ldots, STFT(n,M-1)], \quad (16)$$

calculated as

$$\mathbf{STFT}_M(n) = \mathbf{W}_M\mathbf{s}_\alpha(n), \quad (17)$$

where $\mathbf{s}_\alpha(n) = [s_\alpha(n), \ldots, s_\alpha(n+M-1)]^T$. The theory is easily extended to the overlapped window case.

Observe that relation

$$\mathbf{STFT}_\alpha = \mathbf{W}\mathbf{s}_\alpha = \mathbf{W}\mathbf{W}_N^{-1}\mathbf{S}_\alpha \quad (18)$$

holds. For proper demodulation parameter $\alpha$, DFT vector $\mathbf{S}_\alpha$ is sparse. Additionally, the DFT vector can be expressed as

$$\mathbf{S}_\alpha = \mathbf{W}_N\mathbf{W}^{-1}. \quad (19)$$

Let us introduce the notation $\mathbf{A} = \mathbf{W}\mathbf{W}_N^{-1}$. Applying the m-D removal procedure described in Section III-A, only a subset of non-removed time-frequency points form the vector of available STFT values, $\mathbf{STFT}_{CS}$. The elements of this vector are $STFT\alpha(i) = STFT(n_i, k_i)$, where $(n_i, k_i) \in \mathbb{N}_A$, being the set of retained time-frequency points after the L-statistics. The available STFT points satisfy

$$\mathbf{STFT}_{CS} = \mathbf{A}_{CS}\mathbf{S}_\alpha, \quad (20)$$

where the CS matrix $\mathbf{A}_{CS}$ is formed from matrix $\mathbf{A}$ omitting the rows corresponding to the eliminated time-frequency points.

For properly found $\alpha$, DFT vector containing demodulated rigid body components, now stationary in nature, is sparse. Vector $\mathbf{STFT}_{CS}$ can be interpreted as the vector of available samples (measurements) in the compressive sensing and sparse signal processing frameworks. According to the compressive sensing theory, the rigid body can be reconstructed solving [11], [13]

$$\min \|\mathbf{S}_\alpha\|_1 \ \text{ subject to } \mathbf{STFT}_{CS} = \mathbf{A}_{CS}\,\mathbf{S}_\alpha. \quad (21)$$

Various approaches can be used to solve this $\ell_1$-norm minimization problem. The existence of the solution has been investigated in [13].

### A. Reconstruction algorithm

To solve (21), orthogonal matching pursuit (OMP) algorithm can be used [14]. Based on the available rigid body points in $\mathbf{STFT}_{CS}$ acting as measurements, exact rigid body coefficients at positions $k \in \mathbb{K}$ are reconstructed. The pseudo-code of the procedure is given next:

$\mathbb{K} = \emptyset, \quad \mathbf{y}_r = \mathbf{STFT}_{CS}$
**for** $i = 1 : K$
  $\mathbf{S}_\alpha = N\mathbf{A}_{CS}^H\mathbf{y}_r$
  $k = \arg\{\max_k |\mathbf{S}_\alpha|\}$
  $\mathbb{K} = \mathbb{K} \cup \{k\}$
  $\mathbf{A}_K = \mathbf{A}_{CS}(:, \mathbb{K})$
  $\mathbf{S} = (\mathbf{A}_K^H\mathbf{A}_K)^{-1}\mathbf{A}_K^H\mathbf{STFT}_{CS}$
  $\mathbf{y}_r = \mathbf{STFT}_{CS} - \mathbf{A}_K\mathbf{S}$
**end**
$\mathbf{S}_{\alpha R} = \mathbf{S}$.

This algorithm is used in numerical examples.

## V. Numerical example

Consider the signal defined as

$$s(n) = \sum_{i=1}^{K} \sigma_{B_i} e^{j2\pi[a(\frac{n}{N})^2 + b_i \frac{n}{N}] + j\varphi_i} + \sum_{i=1}^{D} \sigma_{R_i} e^{jA_{R_i} \sin(\omega_{R_i} n + \Theta_i) + j2\pi c_i \frac{n}{N} + j2\pi d_i (\frac{n}{N})^2}. \quad (22)$$

This signal corresponds to a range bin of a radar image. The first summation is a model of rigid body reflectors with non-compensated acceleration $a$. The m-D is modeled with the second summation. Signal length is $N = 1024$.

In our numerical example, we consider the rigid body with $K = 4$ components. The component parameters are given next: $\sigma_{B_i} = [1, 0.5, 1.5, 1]$, $b_i = [125, -125, 245, -255]$ and $\varphi_i = [0, 0, \pi/4, -\pi/3]$ for $i = 1, 2, 3, 4$, respectively. The unknown chirp rate is $a = 360$. The m-D consists of two components, $D = 2$, and the m-D parameters are: $\sigma_{R_i} = [7, 5]$, $\Theta_i = [0, \pi/2]$, $A_{R_i} = [90, 160]$, $\omega_{R_i} = [2.5, 1.95]$, $c_i = [0, 0]$ and $d_i = [0, 0]$, for $i = 1, 2$, respectively. First, we perform the L-statistics based separation of rigid body and m-D, using the procedure described in Section III-A. The demodulation (dechirp) parameter $\alpha = 280$ is obtained using the algorithm presented in Section III-B. The results are presented in Fig. 1. The initial signal STFT, calculated with window length $M = 128$ is shown in Fig. 1a, whereas the corresponding sorted values are given in Fig. 1c. The STFT of the signal dechirped with optimal $\alpha$ is presented in Fig. 1b. and the corresponding sorted STFT values are given in Fig. 1d. The FT of the original signal is presented in Fig. 1e. The STFT-based rigid body and m-D separation does not produce satisfactory results, because significant rigid body parts are removed, as the components are chirps. The FT reconstructed summing $Q = 40\%$ the lowest absolute values of the sorted STFT from Fig. 1d is shown in Fig. 1g. The FT reconstructed summing sorted STFT values according to (8) is shown in Fig. 1h. This example illustrates the fact that the rigid body reconstruction using (8) produces highly concentrated peaks. However, in this paper our aim is to improve the results using the compressed sensing and sparse signal processing framework. The non-overlapped STFT of the signal $s_\alpha(n)$ dechirped using the optimal $\alpha$ is shown in Fig 2a. The window length is $M = 32$. The L-statistics from Section III-A approach is performed on this STFT, removing $U = 40\%$ time-frequency points with largest values, and $D = 20\%$ of points with lowest values. After the m-D removal, the problem (21) is solved using the OMP algorithm presented in Section IV-A. The reconstruction results are shown in Fig. 2e. To emphasize the accuracy of the approach, we present the the STFTs of the original rigid body defined by (22) in Fig. 2c, and the non-compensated rigid body obtained calculating the STFT of the inverse DFT of coefficients presented in Fig. 2e, modulated using the optimal $\alpha$.

## VI. Conclusion

In this paper we consider the separation of rigid body from m-D in case when target acceleration is not compensated. The unknown compensation parameter is found using a simple iterative procedure, based on the LPFT. Applying the compressed sensing (sparse signal reconstruction) concepts, we were able to reconstruct the rigid body using the OMP algorithm, based on time-frequency points remaining after the m-D removal. Our further research is oriented towards the development of algorithm being able to reconstruct the rigid body components which have different chirp rate parameters.

## References


[1] L. Stanković, M. Daković, T. Thayaparan, and V. Popović-Bugarin, "Micro-Doppler Removal in the Radar Imaging Analysis" *IEEE Trans. on Aerospace and El. Sys.*, Vol. 49, No. 2, April 2013, pp.1234–1250

[2] M. Martorella, "Novel approach for ISAR image cross-range scaling," *IEEE Transactions on Aerospace and Electronic Systems*, vol. 44, no. 1, pp. 281-294, January 2008.

[3] M. Brajović, L. Stanković, and M. Daković, "Micro-Doppler removal in radar imaging in the case of non-compensated rigid body acceleration," *2018 23rd International Scientific-Professional Conference on Information Technology (IT)*, Zabljak, Montenegro, 2018, pp. 1-4, February 19-24, doi: 10.1109/SPIT.2018.8350451

[4] V. C. Chen, F. Li, S. S. Ho and H. Wechsler, "Analysis of micro-Doppler signatures," *in IEE Proceedings – Radar, Sonar and Navigation*, vol. 150, no. 4, pp. 271-6-, 1 Aug. 2003.

[5] V. C. Chen, F. Li, S. S. Ho and H. Wechsler, "Micro-Doppler effect in radar: phenomenon, model, and simulation study," *in IEEE Trans. on Aerospace and El. Sys.*, vol. 42, no. 1, pp. 2-21, Jan. 2006.

[6] X. Bai, F. Zhou, M. Xing and Z. Bao, "High Resolution ISAR Imaging of Targets with Rotating Parts textquotedblright *in IEEE Transactions on Aerospace and Electronic Systems*, vol. 47, no. 4, pp. 2530-2543, Oct 2011.

[7] J. Li and H. Ling, "Application of adaptive chirplet representation for ISAR feature extraction from targets with rotating parts," *in IEE Proc. - RSN*, vol. 150, no. 4, pp. 284–91, 1 Aug. 2003.

[8] Y. Wang, Y.-C. Jiang, "ISAR imaging of ship target with complex motion based on new approach of parameters estimation for polynomial phase signal," *EURASIP Journal on Advances in Signal Processing* 2011(2011) ArticleID 425203, 9 pp.

[9] L. Stanković, M. Daković and T. Thayaparan, *Time–Frequency Signal Analysis with Application*, Artech House, 2013

[10] B. Boashash, *Time-Frequency Signal Analysis and Processing –A Comprehensive Reference*, Elsevier Science, Oxford, 2003.

[11] L. Stanković, I. Orović, S. Stanković, and M. Amin, "Compressive Sensing Based Separation of Non-Stationary and Stationary Signals Overlapping in Time-Frequency," *IEEE Transactions on Signal Processing*, Vol. 61, no. 18, pp. 4562 — 4572, Sept. 2013

[12] L. Stanković, "A measure of some time-frequency distributions concentration," *Signal Processing*, vol. 81, pp. 621–631, Mar. 2001

[13] L. Stanković, S. Stanković, T. Thayaparan, M. Daković, and I. Orović, "Separation and Reconstruction of the Rigid Body and Micro-Doppler Signal in ISAR Part I – Theory" *IET Radar, Sonar & Navigation*, vol.9, no.9, pp.1147-1154, 2015

[14] D. Needell, J. A. Tropp, "CoSaMP: Iterative signal recovery from incomplete and inaccurate samples," Applied and Computational Harmonic Analysis, vol. 26, no. 3, pp. 301–321, 2009.

[15] D. L. Donoho, "Compressed sensing," IEEE Trans. Information Theory, vol. 52, no. 4, pp. 1289–1306, 2006.

[16] E. J. Candès, M. B. Wakin, "An Introduction to Compressive Sampling," *IEEE Signal Processing Magazine*, vol. 21, March 2008.

[17] E. J. Candes, J. Romberg, T. Tao, "Robust uncertainty principles: exact signal reconstruction from highly incomplete frequency information," *IEEE Trans. on Inform. Theory*, vol. 52, no. 2, pp. 489–509, Feb. 2006.

[18] I. Volarić, V. Sučić, Z. Car, "A compressive sensing based method for cross-terms suppression in the time-frequency plane," *IEEE 15th International Conference on Bioinformatics and Bioengineering*, pp. 1–4, 2015.